PAPER

Check for updates

Rational design of elastin-like polypeptide fusion proteins to tune self-assembly and properties of protein vesicles†

Yirui Li,‡[ab] Dylan R. Dautel,‡[a] Mikaela A. Gray, [ID] ‡[a] Michael E. McKenna[a] and Julie A. Champion [ID] ⋆[ab]

Protein vesicles made from bioactive proteins have potential value in drug delivery, biocatalysis, and as artificial cells. As the proteins are produced recombinantly, the ability to precisely tune the protein sequence provides control not possible with polymeric vesicles. The tunability and biocompatibility motivated this work to develop protein vesicles using rationally designed protein building blocks to investigate how protein sequence influences vesicle self-assembly and properties. We have reported an elastin-like polypeptide (ELP) fused to an arginine-rich leucine zipper (Z_R) and functional, globular proteins fused to a glutamate-rich leucine zipper (Z_E) that self-assemble into protein vesicles when warmed from 4 to 25 °C due to the hydrophobic transition of ELP. Previously, we demonstrated the ability to tune vesicle properties by changing protein and salt concentration, Z_E:Z_R ratio, and warming rate. However, there is a limit to the properties that can be achieved *via* assembly conditions. In order to access a wider range of vesicle diameter and stability profiles, this work investigated how modifiying the hydrophobicity and length of the ELP sequence influenced self-assembly and the final properties of protein vesicles using mCherry as a model globular protein. The results showed that both transition temperature and diameter of protein vesicles were inversely correlated to the ELP guest residue hydrophobicity and the number of ELP pentapeptide repeats. Additionally, sequence manipulation enabled assembly of vesicles with properties not accessible by changes to assembly conditions. For example, introduction of tyrosine at 5 guest residue positions in ELP enabled formation of nanoscale vesicles stable at physiological salt concentration. This work yields design guidelines for modifying the ELP sequence to manipulate protein vesicle transition temperature, size and stability to achieve desired properties for particular biofunctional applications.

Introduction

Elastin-like polypeptides (ELPs) are biopolymers derived from human tropoelastin.[1,2] ELPs are composed of the pentapeptide repeat (VPGXG)$_n$, where the guest residue is represented by X and n represents the number of repeats. ELPs are thermo-responsive and exhibit lower critical solution temperature phase behaviour. When heated above their transition temperature (T_t), ELPs undergo inverse-phase transition from soluble to insoluble with a hydrophobic conformational change that induces coacervation.[1,3,4] T_t depends on protein length n,[5] concentration of ELP[5] and salts,[6,7] and guest residue composition.[8] Modifications in guest residue have been used to tune ELP hydrophobicity,[8] incorporate stimuli-responsiveness,[9,10] and enable crosslinking.[11] Given these properties, ELPs are attractive for fabricating biomaterials due to their thermoresponsiveness, ability to self-assemble, and highly tunable phase transition behaviour. Self-assembling ELP-based nanoparticles have been developed with diverse properties for biomedical applications.[12–15]

Our group has previously reported protein vesicles as a novel self-assembling ELP-based micro/nanoparticle.[16] While the vesicles resemble protein cages as hollow structures made of proteins, their building blocks and mode of assembly are quite different. The vesicle building blocks are an ELP fused to an arginine-rich leucine zipper (Z_R), Z_R-ELP, and a hydrophilic, globular protein fused to a glutamic acid-rich leucine zipper (Z_E).[16,17] Z_E fused to globular proteins, such as enzymes or model fluorescent mCherry protein (*i.e.* mCherry-Z_E) binds

[a] *School of Chemical and Biomolecular Engineering, Georgia Institute of Technology, 950 Atlantic Drive NW, Atlanta, Georgia, 30332, USA. E-mail: julie.champion@chbe.gatech.edu*

[b] *BioEngineering Program, Georgia Institute of Technology, 950 Atlantic Drive NW, Atlanta, Georgia, 30332, USA*

† Electronic supplementary information (ESI) available. See DOI: https://doi.org/10.1039/d3tb00200d

‡ Co-first authors.

This journal is © The Royal Society of Chemistry 2023

J. Mater. Chem. B, 2023, **11**, 6443–6452 | **6443**

strongly to Z_R in Z_R-ELP to create a protein amphiphile upon warming.[18,19] Protein vesicles self-assemble from the fusion proteins above a critical salt concentration, temperature and $Z_E : Z_R$ molar ratio. In previous work the Z_R-ELP protein has 25 ELP pentapeptide repeats of the amino acid sequence, VPGXG, where the X guest residues are valine (20) and phenylalanine (5). We have shown that salt concentration plays an important role in the self-assembly of protein vesicles due to its impact on the T_t of ELP.[18,19] In order to prepare stable vesicles from mCherry-Z_E and the original Z_R-ELP design, the critical salt concentration needed to be at least twice that of physiological conditions (≥ 0.30 M NaCl) and the vesicles that formed were micron-sized, depending on the molar ratio and protein concentration.[16] High salt concentrations (>1.0 M NaCl) were necessary to form nanoscale protein vesicles and UV cross-linking was required for stabilization in physiological salt concentration for biomedical applications.[19] However, for applications such as drug delivery, artificial cells and biocatalysis, the buffer conditions and temperature are fixed and each application has different desired size requirements and globular proteins fused to Z_E. Additionally, UV crosslinking is not ideal as it can damage the structure of the globular protein or nucleic acid or protein cargos.[20,33]

To make protein vesicles more versatile for bioengineering applications and overcome the limits of manipulating self-assembly conditions, we propose to modify the ELP sequence to tune the phase transition, self-assembly and properties of protein vesicles. According to Urry et al., the hydrophobicity of amino acid residues in ELP scales from most to least hydrophobic: Trp, Tyr, Phe, Ile–Leu–Met, Val, Ala, and Gly.[21] When these residues are substituted into ELP as guest residues, the T_t inversely depends on the mean hydrophobicity and the heat of transition directly depends on the mean residue hydrophobicity.[8] Simulation of the conformational transition as a function of guest residue hydrophobicity supports the experimental observations.[22] Furthermore, when the number of ELP pentapeptide repeats increases, the T_t decreases.[1,5,23] Theoretically, increasing hydrophobicity of the ELP residues and the number of pentapeptide repeats should lead to a higher interfacial tension between ELP and water. According to the classical descriptions of amphiphile packing, that would lead to a more negative free energy when ELP transitions from water soluble to an aggregate or coacervate structure and should improve the favourability of vesicle self-assembly.[24,25] Therefore, we hypothesize that it is possible to tailor the self-assembly and properties of protein vesicles by varying ELP sequence to increase the range of properties to be useful for more applications.

In this work, we modified the ELP guest residue hydrophobicity and length in Z_R-ELP to tune the vesicle self-assembly and properties (Table 1 and Table S1, ESI†). Valine was substituted with more hydrophobic isoleucine (I) and tyrosine (Y) residues at 5, 10, and 15 positions while keeping the original ELP length of 25 repeats. The number of pentapeptide repeats was varied from 25 to 15, 35, and 50. The results presented here expand the range of critical T_t and NaCl concentrations available for protein vesicle formation, reveal the strong correlation

Table 1 ELP sequence variants used in this work

ELP Name	ELP Sequence
Z_R-ELP (Z_R-ELP$_{25}$)	[VPGVG VPGVG VPGFG VPGVG VPGVG]$_5$
I$_5$-Z_R-ELP	[VPGVG VPG**I**G VPGFG VPGVG VPGVG]$_5$
I$_{10}$-Z_R-ELP	[VPGVG VPG**I**G VPGFG VPG**I**G VPGVG]$_5$
I$_{15}$-Z_R-ELP	[VPG**I**G VPG**I**G VPGFG VPG**I**G VPGVG]$_5$
Y$_5$-Z_R-ELP	[VPGVG VPG**Y**G VPGFG VPGVG VPGVG]$_5$
Y$_{10}$-Z_R-ELP	[VPGVG VPG**Y**G VPGFG VPG**Y**G VPGVG]$_5$
Y$_{15}$-Z_R-ELP	[VPG**Y**G VPG**Y**G VPGFG VPG**Y**G VPGVG]$_5$
Z_R-ELP$_{15}$	[VPGVG VPGVG VPGFG VPGVG VPGVG]$_3$
Z_R-ELP$_{35}$	[VPGVG VPGVG VPGFG VPGVG VPGVG]$_7$
Z_R-ELP$_{50}$	[VPGVG VPGVG VPGFG VPGVG VPGVG]$_{\underline{10}}$

between T_t and diameter, and provide a genetic handle for tuning vesicle diameter and stability at given process conditions. This ability to rationally tune vesicle diameter with simple sequence changes known in the ELP literature to control T_t sets it apart from traditional protein cages where symmetry and oligomeric state must be altered in order to change size and there are no obvious mutations known to enable facile control of cage size.[26,27]

Results and discussion

Isoleucine ELP variants reduced T_t and vesicle diameter

Each isoleucine variant (I-Z_R-ELP) was expressed in *E. coli* and purified *via* affinity chromatography (Fig. S1, ESI†). After confirming protein purity by gel electrophoresis, the transition temperature (T_t) of each mCherry-Z_E/I-Z_R-ELP mixture was measured by turbidimetry as a function of NaCl concentration to determine the effect of the guest residue on T_t of the ELP. The transition temperature was measured by mixing I-Z_R-ELP with mCherry-Z_E (30 μM I-Z_R-ELP and 1.5 μM mCherry-Z_E, used in all experiments, typical of previous work) on ice in solutions containing 0.15, 0.30, 0.50, or 1.0 M NaCl. Then, the turbidity of the solution was measured every minute as the temperature was increased from 4 °C to 50 °C at a ramp rate of 1 °C min^{-1}. The transition temperature was recorded to be the inflection point of these turbidity vs temperature profiles (Fig. S2, ESI†). Consistent with previous literature substituting isoleucine in the guest residue,[8,21] the T_t of each I-Z_R-ELP mixture was reduced as the number of isoleucine guest residues and NaCl concentration increased (Fig. 1). In the case of mCherry-Z_E/I$_{10}$-Z_R-ELP and I$_{15}$-Z_R-ELP mixtures at 1.0 M NaCl, T_t could not be measured because it was below the limit of the instrument. The reduction in T_t with increasing salt can be explained by a loss of waters that contribute to hydrophobic hydration of ELP at elevated NaCl concentration.[6] When the isoleucine content was higher, T_t decreased due to increased hydrophobicity of ELP.[15] However, hydrophobicity is likely not the only factor. T_t of ELPs with valine *versus* isoleucine guest residues does not clearly correlate with their calculated partition coefficient, suggesting that side chain conformation may be important as well as hydrophobicity.[28] We also observed that the effect of isoleucine addition did saturate. For instance, the T_t of I$_{15}$-Z_R-ELP was only slightly lower than for I$_{10}$-Z_R-ELP, whereas the differences in T_t of Z_R-ELP and I$_5$-Z_R-ELP compared to I$_{10}$-Z_R-ELP
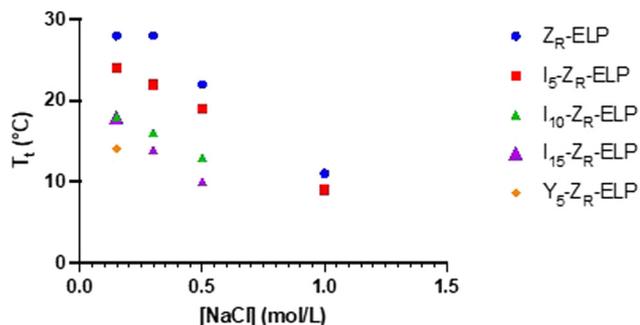
6444 | *J. Mater. Chem. B*, 2023, **11**, 6443–6452

This journal is © The Royal Society of Chemistry 2023

Fig. 1 Transition temperature measurements as a function of salt concentration for 30 µM Z_R-ELP, I_5-Z_R-ELP, I_{10}-Z_R-ELP, I_{15}-Z_R-ELP, and Y_5-Z_R-ELP mixed with 1.5 µM mCherry-Z_E.

were much larger. Increasing salt reduces the differences between the Z_R-ELP and I_5-Z_R-ELP variants above 0.15 M. This trend was also expected between the isoleucine variants, but was not observed.

After demonstrating the decrease in T_t of I-Z_R-ELPs with increasing guest residue hydrophobicity, we sought to determine if the guest residue hydrophobicity altered vesicle self-assembly conditions and properties. Vesicle formation was initiated by mixing mCherry-Z_E with I-Z_R-ELP on ice at NaCl concentrations of 0.15, 0.30, 0.50, and 1.0 M and then incubating at 25 °C for one hour while monitoring turbidity. The structures that formed were characterized by epifluorescence microscopy. Vesicle formation was confirmed for salt concentrations above 0.15 M NaCl for each of the I-Z_R-ELP variants, evidenced by both stable turbidity profiles (Fig. 2) and microscopy (Fig. 3 and Fig. S3, ESI†). At NaCl concentrations of 0.15 M, Z_R-ELP and I_5-Z_R-ELP were not able to transition from coacervates to vesicles and coacervates with unstable turbidity profiles remained the dominant structures.

Also, at 0.15 M NaCl, I_{10}-Z_R-ELP and I_{15}-Z_R-ELP exhibited clusters of microparticles, and while they appeared to be stable, microscopy did not reveal any vesicle morphology.

Vesicle size was quantified by dynamic light scattering (DLS) and followed the same trend with isoleucine content as T_t (Fig. 4a), namely increasing isoleucine content and increasing salt concentration both decreased vesicle size. However, like T_t, the effect saturated and vesicles made from I_{10}-Z_R-ELP and I_{15}-Z_R-ELP had similar diameters at all NaCl concentrations. Additionally, at 1.0 M NaCl the effect of salt dominated and all vesicles exhibited similar nanoscale diameters, though they were still correlated with isoleucine content (Z_R-ELP 254 $\pm$ 78 nm, I_5-Z_R-ELP 257$\pm$ 7.9 nm, I_{10}-Z_R-ELP 231$\pm$ 33 nm, I_{15}-Z_R-ELP 192 $\pm$ 6.3 nm). The reduction in vesicle size with increased hydrophobicity could be attributed to a reduction in the amount of time spent in the coacervate phase. As the temperature of the mixture rises from 4 to 25 °C, the ELP transitions from soluble to coacervate and then from coacervate to vesicles. Although the coacervate stage is transient, the time that the proteins spend in the coacervate phase affects vesicle size.[29] In the coacervate phase, the particles do not have a strong boundary and there is dynamic exchange between the soluble protein and the coacervates. This allows coacervates to coalesce and grow until they are kinetically trapped as the continued increase in temperature and ELP hydrophobicity leads to reorganization of coacervates into vesicles. The stable membrane structure of vesicles and lack of remaining soluble Z_R-ELP prohibits growth once vesicles form. The turbidity profiles of vesicles show that as the isoleucine content is increased, the vesicles spend less time transitioning from soluble protein to coacervate (high positive slope region of profile, Fig. 2) and then to vesicles. Therefore, the vesicles are
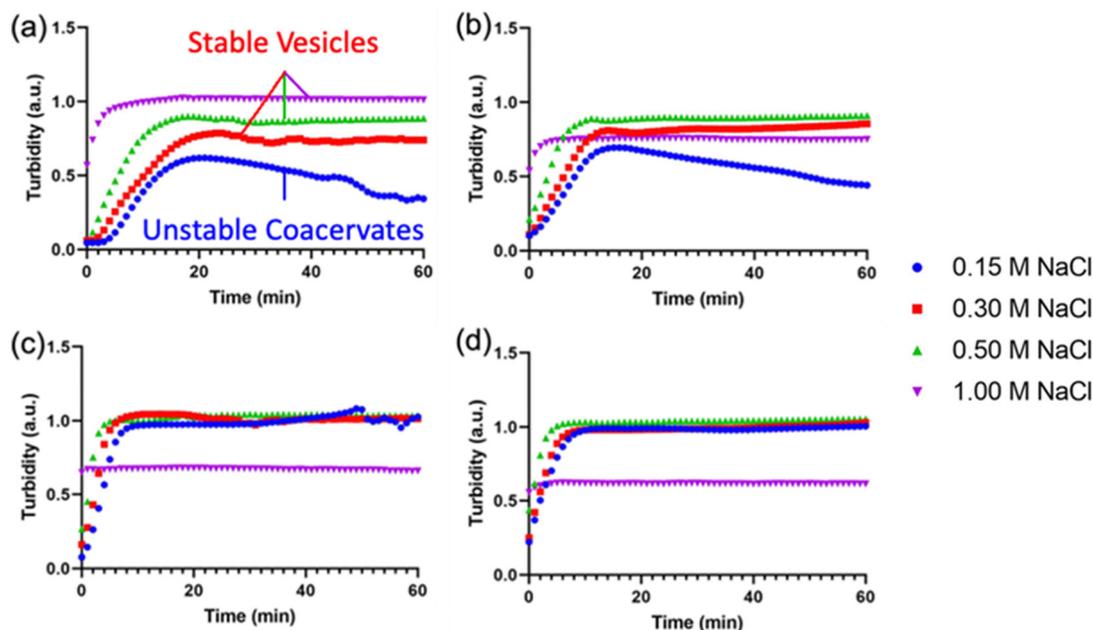

Fig. 2 Turbidity profiles of mCherry-Z_E/I-Z_R-ELP upon warming to 25 °C at 0.15, 0.30, 0.50, and 1.0 M NaCl. Turbidity profiles of (a) Z_R-ELP, (b) I_5-Z_R-ELP, (c) I_{10}-Z_R-ELP, and (d) I_{15}-Z_R-ELP.

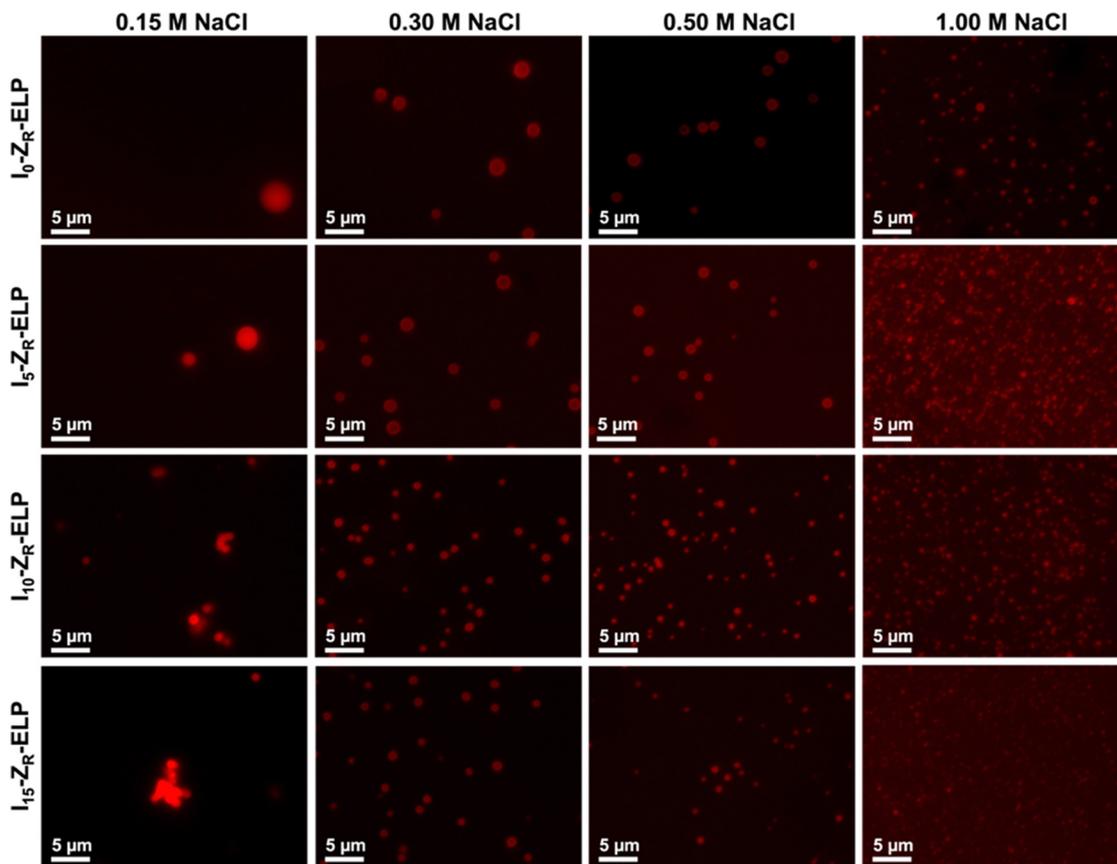This journal is © The Royal Society of Chemistry 2023

J. Mater. Chem. B, 2023, 11, 6443–6452 | 6445

Fig. 3 Epifluorescence micrographs of structures made from mixing 1.5 μM mCherry-Z_E and 30 μM Z_R-ELP, I_5-Z_R-ELP, I_{10}-Z_R-ELP, or I_{15}-Z_R-ELP at 0.15, 0.30, 0.50, and 1.0 M NaCl and warming from 4 to 25 °C for one hour. See Fig. S3 (ESI†) for enlarged insets.
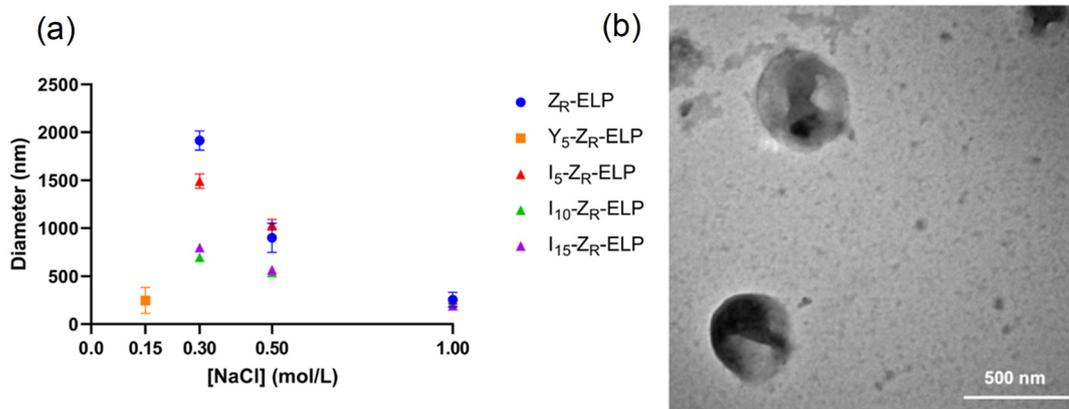

Fig. 4 Characterization of mixtures of mCherry-Z_E with I-Z_R-ELP or Y-Z_R-ELP as a function of NaCl concentration. (a) Hydrodynamic diameters of mCherry-Z_E/I-Z_R-ELP and mCherry-Z_E/Y_5-Z_R-ELP and using 30 μM Z_R-ELP and 1.5 μM mCherry-Z_E at varying salt concentrations. Error bars represent standard deviation of average diameter and are too small to be seen for some measurements. (b) Representative TEM image of I_{15}-Z_R-ELP vesicles assembled in 1.0 M NaCl.

likely smaller because of the short time spent in the coacervate stage. The smallest vesicles formed at 1.0 M NaCl from mCherry-Z_E/I_{15}-Z_R-ELP nearly instantaneously, faster than our ability to measure the turbidity increase. The nanoscale vesicle structure was confirmed by TEM (Fig. 4b). The role of time

spent in the transition on vesicle size was corroborated by changing the heating rate of protein solution, which is an alternate method of changing the time in the coacervation stage. Vesicles made with mCherry-Z_E/I_{15}-Z_R-ELP at 0.5 M NaCl were much smaller when warmed at 5 °C min^{-1} than at

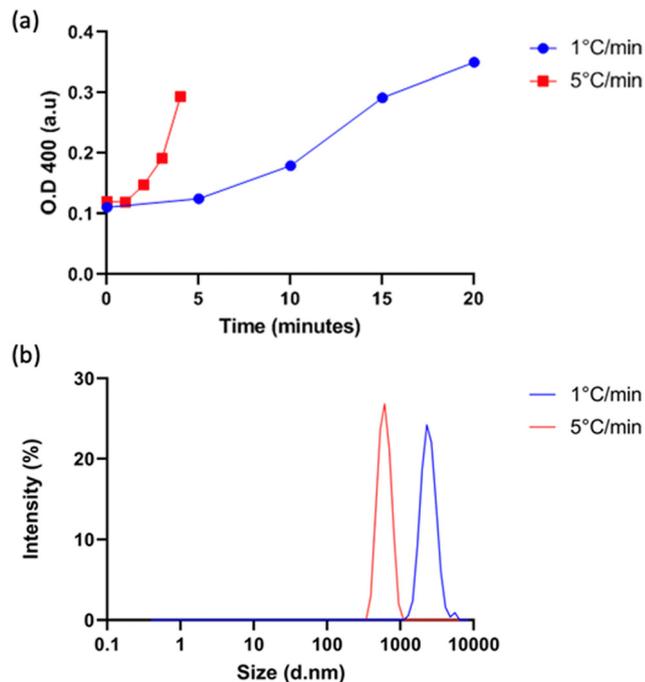6446 | *J. Mater. Chem. B*, 2023, **11**, 6443–6452

This journal is © The Royal Society of Chemistry 2023

Fig. 5 Characterization of vesicles made with slower (1 °C min^{-1}) and faster (5 °C min^{-1}) warming of 5 to 25 °C from 1.5 μM mCherry-Z_E and 30 μM I_{15}-Z_R-ELP with 0.5M NaCl. (a) Turbidity profiles of protein mixtures and (b) hydrodynamic diameters of vesicles formed with varied heating rates.

1 °C min^{-1} (Fig. 5 and Fig. S4, ESI†). It should also be noted that each ELP contains one terminal cysteine (Table S1, ESI†) that can form a disulfide bond with another ELP. These may also constrain and slow protein reorganization from coacervate to vesicle. Preventing disulfide bonds by capping the cysteine thiols with aldrithiol resulted in significantly smaller vesicles (216.3 ± 1.71 nm compared to 605.9 ± 11.4 nm for mCherry-Z_E/I_{15}-Z_R-ELP at 0.5 M NaCl, Fig. S5, ESI†).

Tyrosine ELP variant reduced T_t, vesicle diameter and minimum required salt concentration

Since I_{10}-Z_R-ELP and I_{15}-Z_R-ELP formed clustered spherical particles at 0.15 M NaCl, demonstrating greater propensity for stable self-assembly than coacervates formed by Z_R-ELP and I_5-Z_R-ELP, we hypothesized that further increasing ELP hydrophobicity could further reduce T_t and may produce stable vesicles. According to the ELP hydrophobicity scale established by Urry *et al.*, tyrosine is the second most hydrophobic amino acid.[21] Therefore, we incorporated hydrophobic tyrosine at guest positions. We employed the same design strategy with 5, 10, and 15 tyrosine substituted to make Y_5-Z_R-ELP, Y_{10}-Z_R-ELP, and Y_{15}-Z_R-ELP, respectively. Y_{15}-Z_R-ELP did not express in *E. coli* despite optimization, but the others did and were purified by affinity chromatography after optimization of lysis buffer (Fig. S1, ESI†).

We performed the same characterization on tyrosine ELP variants as for isoleucine. However, when proteins were mixed on ice at different salt concentrations and warmed to 25 °C, it was apparent that mCherry-Z_E/Y_5-Z_R-ELP at 0.50 and 1.0 M NaCl and Y_{10}-Z_R-ELP protein mixtures at all salt concentrations started phase transitioning on ice. Therefore, most turbidity profiles did not capture the transition and it was not possible to measure T_t. Only the T_t of mCherry-Z_E/Y_5-Z_R-ELP at 0.15 M NaCl was able to be measured, as 14 °C (Fig. 1 and Fig. S2, ESI†). This large decrease in mCherry-Z_E/Y_5-Z_R-ELP T_t compared to mCherry-Z_E/I_5-Z_R-ELP T_t is in agreement with literature that observed a 65 °C drop for ELPs with 100% tyrosine guest residues compared to 100% isoleucine guest residues and a 15 °C drop for 20% isoleucine guests switched to 20% tyrosine (remaining 80% guest valine) but only a 10 °C or 5 °C decrease in T_t when switching from valine to isoleucine for 100% or 20%, respectively.[8,21] Though the sequences and conditions are not the same, in our design 20% of the guest residues are also
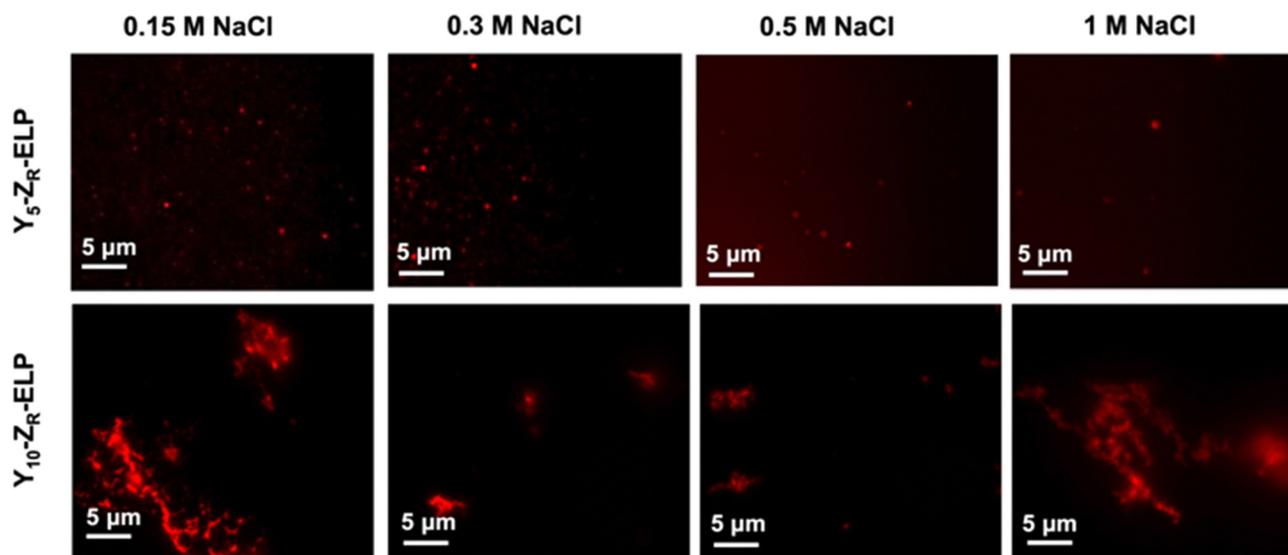

Fig. 6 Epifluorescence micrographs of structures made from mixing 1.5 μM mCherry-Z_E and 30 μM Y_5-Z_R-ELP or Y_{10}-Z_R-ELP at 0.15, 0.30, 0.50, and 1.0 M NaCl and warming from 4 to 25 °C for one hour.

This journal is © The Royal Society of Chemistry 2023

J. Mater. Chem. B, 2023, **11**, 6443–6452 | **6447**

varied. The relative trend observed of 10 °C decrease in T_t for isoleucine to tyrosine and only 4 °C for valine to isoleucine is consistent. Analysis of the turbidity profiles revealed that only mCherry-Z_E/Y_5-Z_R-ELP at 0.3 M NaCl exhibited a vesicle-like turbidity profile that was stable after the initial increase (Fig. S6, ESI†). Epifluorescence (Fig. 6) and TEM (Fig. 7 and Fig. S7, ESI†) micrographs and DLS (Fig. 4a) revealed much more information about the structures. Y_5-Z_R-ELP formed nanoscale vesicles at 0.15 M, as confirmed by TEM. Stable nanoscale structures formed at 0.30 M NaCl also, although TEM showed high internal density suggesting these were stable vesicle-coacervate hybrids, where a dense coacervate phase exits stably within a vesicle-like shell with enriched mCherry-Z_E at the perimeter.[18] DLS reported a diameter of 248.2 ± 6.35 nm with a polydispersity index of 0.154 ± 0.015 for mCherry-Z_E/Y_5-Z_R-ELP vesicles assembled at 0.15 M. For higher salt concentrations, larger vesicle coacervate hybrids and coacervates were evident in mCherry-Z_E/Y_5-Z_R-ELP fluorescence and TEM images although stable DLS data could not be obtained. The final structures of mCherry-Z_E/Y_{10}-Z_R-ELP complexes at all NaCl concentrations were clustered solid particles. The fact that vesicles only formed for Y_5-Z_R-ELP vesicles 0.15 M NaCl and hybrid or aggregated, non-vesicular structures formed at higher salt or greater tyrosine content indicate that too much hydrophobicity in the ELP domain can lead to an imbalance in protein amphiphile packing during self-assembly. This highlights the importance of designing protein amphiphiles with a balanced hydrophilic/hydrophobic ratio for vesicle formation.

In comparing the isoleucine and tyrosine variants, the most striking difference was the reduction in minimum salt concentration required to form vesicles. The T_t of Y_5-Z_R-ELP vesicles at its lower critical salt concentration, 0.15 M NaCl, was 14 °C while the T_t of I_5, I_{10}, and I_{15}-Z_R-ELP vesicles at their lower critical salt concentration, 0.30 M NaCl, was 22 °C, 15 °C, and 13 °C, respectively. This effect was likely caused by π–π stacking interactions from the phenolic group in tyrosine that further enhanced the hydrophobic effect.[30] Work by Taylor *et al.* demonstrated that substitution of phenylalanine with tyrosine at the guest residue position in ELP led to a reduction in T_t.[31]
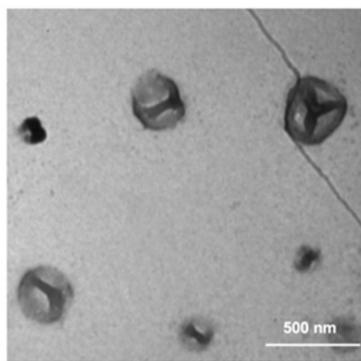

Fig. 7 TEM image of structures made from mixing 1.5 μM mCherry-Z_E and 30 μM Y_5-Z_R-ELP at 0.15 M NaCl and warming from 4 to 25 °C for one hour.

Their simulation data suggested that increased π–π stacking interactions between tyrosines were responsible. Lower T_t reflects a decrease in endothermic heat required to destructure the water molecules of hydrophobic hydration organized around ELP prior to the transition.[8] This is an example where sequence tuning could enable an application such as drug delivery since the Y_5-Z_R-ELP variant forming nanoscale vesicles at physiological salt concentration (phosphate buffered saline (PBS) contains 149.7 mM total salt). These vesicles were stable when the protein concentration was diluted with PBS, even though reducing protein concentration increases T_t,[17] demonstrating that strong Y_5-Z_R-ELP protein-protein interactions maintain the high local protein concentration in the vesicle membrane and suggest these vesicles could be used in drug delivery applications (Fig. S8, ESI†).

Increasing ELP length decreased T_t and vesicle size

The number of pentapeptide repeats also affects the T_t of ELP. When ELP is lengthened, the T_t typically decreases.[1,5] In order to determine the effect of increasing the number of pentapeptide repeats of ELP on vesicle self-assembly we designed three variants of Z_R-ELP with 15, 35, and 50 pentapeptide repeats termed Z_R-ELP$_{15}$, Z_R-ELP$_{35}$, and Z_R-ELP$_{50}$ and compared these to the original (Z_R-ELP$_{25}$). All proteins were expressed in *E. coli* and purified by affinity chromatography (Fig. S1, ESI†).

To determine the effect of ELP length on vesicle self-assembly we performed the same characterization as for hydrophobic variants. First, we measured the T_t by turbidimetry of mCherry-Z_E/Z_R-ELP mixtures of 1.5 μM mCherry-Z_E and 30 μM Z_R-ELP in 0.15 M, 0.30 M, 0.50 M, and 1.0 M NaCl (Fig. 8a). As ELP length increased, T_t fell, as observed in previous literature.[1,5,23] Interestingly, the salt concentration played a smaller role in the T_t of shorter ELPs at lower salt concentrations. The shorter variants experienced no depression in T_t when salt concentration was increased from 0.15 to 0.50 M NaCl for Z_R-ELP$_{15}$ or 0.15 to 0.30 M for Z_R-ELP$_{25}$. Conversely, the T_t of Z_R-ELP$_{35}$ and Z_R-ELP$_{50}$ both fell with each salt concentration increase. The T_t of Z_R-ELP$_{35}$ and Z_R-ELP$_{50}$ was too low to measure at 1.0 M NaCl as those variants begin to transition immediately upon addition of NaCl at 5 °C.

Next, mCherry-Z_E and each Z_R-ELP$_n$ variant were mixed on ice with NaCl and incubated at 25 °C to form vesicles. Turbidity profiles indicated that Z_R-ELP$_{15}$ exhibited a very weak transition with only a small increase in turbidity at low salt and a stable, fully transitioned vesicle profile was only apparent at 1.0 M NaCl (Fig. S9, ESI†). This is likely because the T_t values with lower salt were greater than 25 °C. Likewise DLS only gave acceptable quality measurements at 1.0 M NaCl (Fig. S10, ESI†). However, epifluorescence microscopy did reveal a small number of coacervates or coacervate-vesicle hybrid structures formed from Z_R-ELP$_{15}$ at 0.30 M and 0.50 M NaCl, although perhaps the concentration was too low to obtain a measurable size by DLS (Fig. 9 and Fig. S10, ESI†). The remaining Z_R-ELP$_n$ variants demonstrated robust turbidity increases upon warming (Fig. S9, ESI†). While the turbidity profile of mCherry-Z_E/Z_R-ELP$_{25}$ at 0.15 M was unstable, the remaining profiles for Z_R-ELP$_{25}$, and all salt concentrations for Z_R-ELP$_{35}$ and Z_R-ELP$_{50}$ were stable, suggesting vesicle assembly. Microscopy

6448 | *J. Mater. Chem. B*, 2023, **11**, 6443–6452

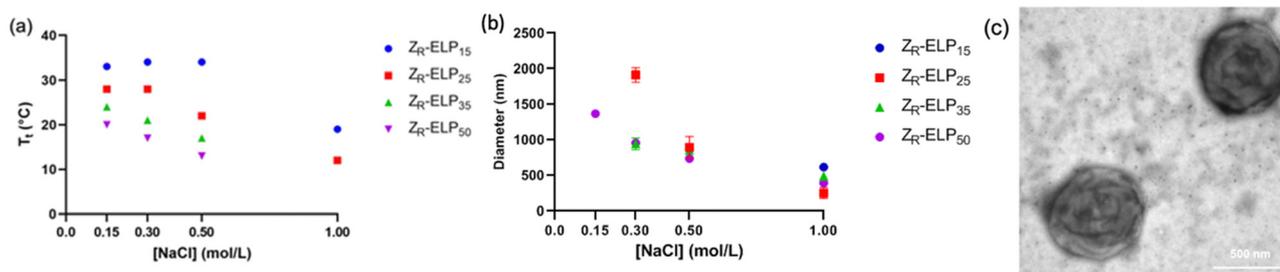This journal is © The Royal Society of Chemistry 2023

Fig. 8 Characterization of mixtures of mCherry-Z_E and Z_R-ELP$_n$ variants as a function of NaCl concentration. (a) T_t and (b) average hydrodynamic diameter of each Z_R-ELP$_n$ variant at 0.15 M, 0.30 M, 0.50, and 1.0 M NaCl. Error bars represent standard deviation of average diameter and are too small to be seen for some measurements. (c) TEM image of Z_R-ELP$_{50}$ vesicles in 1.0 M NaCl.
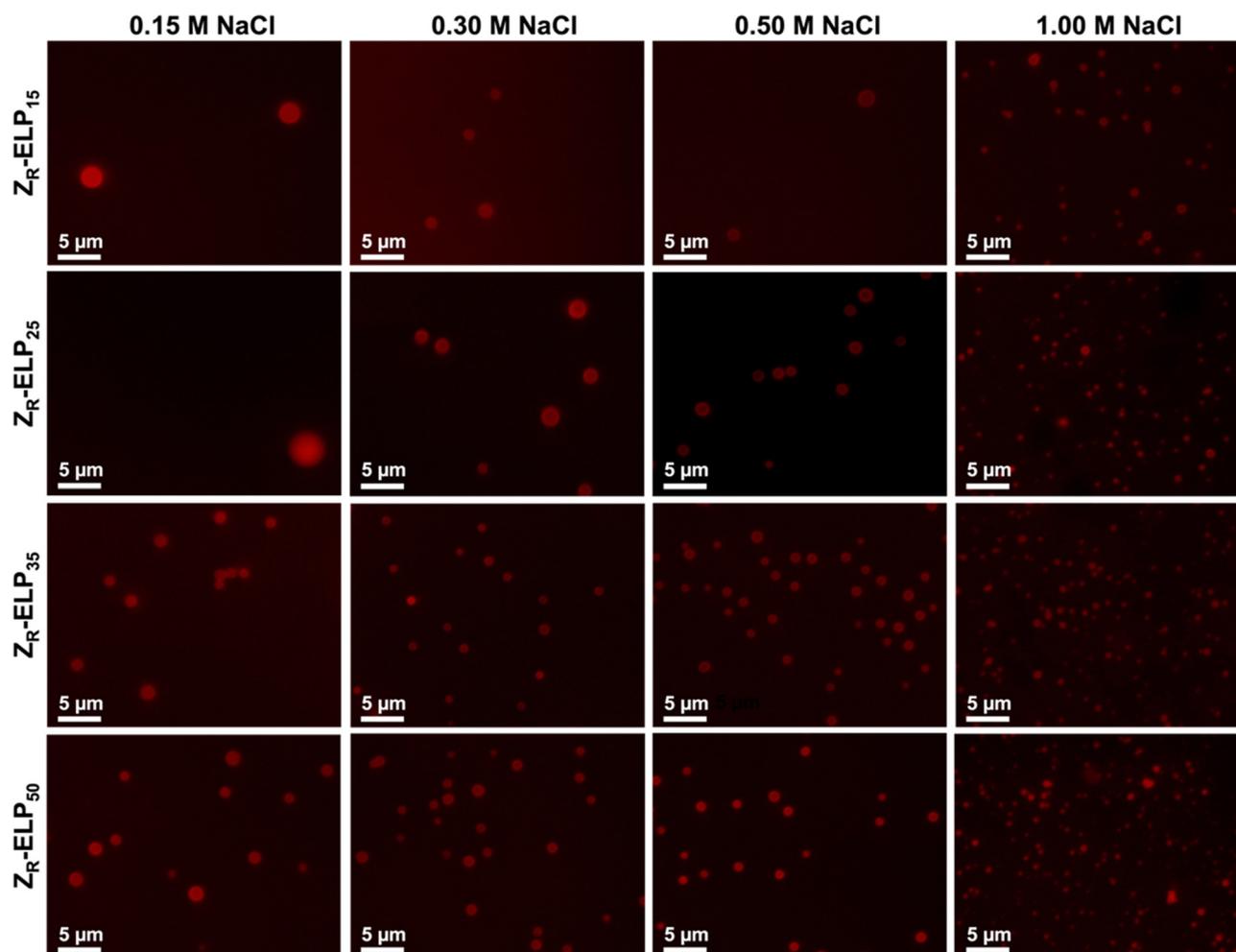

Fig. 9 Epifluorescence micrographs of structures made from mixing 1.5 μM mCherry-Z_E and 30 μM Z_R-ELP$_{15}$, Z_R-ELP$_{25}$, Z_R-ELP$_{35}$, or Z_R-ELP$_{50}$ at 0.15, 0.30, 0.50, and 1.0 M NaCl and warming from 4 to 25° for one hour. See Fig. S11 (ESI†) for enlarged insets.

confirmed vesicle formation for all stable profiles with the exception of 0.15 M NaCl (Fig. 9 and Fig. S11, ESI†). At 0.15 M NaCl Z_R-ELP$_{35}$ and Z_R-ELP$_{50}$ mixed with mCherry-Z_E exhibited distinct vesicle-like ring structures that also contained red fluorescent mCherry-Z_E protein in the interior region of the particles, which are vesicle-coacervate hybrids that have

properties of both coacervates and vesicles.[19] The average hydrodynamic diameter of the self-assembled structures was measured with DLS (Fig. 8b). As with I-Z_R-ELP, the T_t of Z_R-ELP$_n$ variants positively correlated with the average hydrodynamic diameter of the vesicles that formed, so ELPs with less repeats tended to result in the formation of larger vesicles. This was

This journal is © The Royal Society of Chemistry 2023

J. Mater. Chem. B, 2023, **11**, 6443–6452 | **6449**

again attributed to the time spent in the transition phase, which was longer for shorter variants and lower NaCl concentrations. As expected, mCherry-Z_E/Z_R-ELP$_{50}$ vesicles formed in 1.0 M salt were smallest, and their structure confirmed by TEM (Fig. 8c). However, the same saturation effect was observed as for isoleucine variants, with a greater difference in average diameter between ELP lengths of 25 and 35 than 35 and 50. Additionally, at high salt the effect of ELP length was significantly diminished.

One important difference between varying the ELP guest residue content and ELP length was the change in hydrophobicity of the pentapeptide repeat. When ELP was lengthened, there is no increase in the hydrophobicity of the pentapeptide repeats although the T_t is reduced. The depression of T_t is likely not caused by enhanced hydrophobicity, but rather could be due to an increase in nucleation sites for oligomerization and coacervation of ELP. The smallest vesicles were made from I$_{15}$-Z_R-ELP at 1.0 M NaCl and Y$_5$-Z_R-ELP at 0.15 M NaCl, which had hydrodynamic diameters of approximately 250 nm and 260 nm, respectively. Meanwhile, the smallest length variant vesicles occurred at 1.0 M NaCl and were approximately double the size, between 550 and 650 nm for Z_R-ELP$_{25}$, Z_R-ELP$_{35}$, and Z_R-ELP$_{50}$. One potential reason that the vesicles made from longer ELPs were considerably larger even at higher salt concentrations could be that the longer ELP chains cannot pack as tightly as shorter ELP chains. Therefore, increased ELP hydrophobicity is a more effective approach to decreasing vesicle size than increasing ELP length, although both decrease T_t.

Conclusions

In this work, we demonstrated that protein vesicle properties can be altered by rational design of Z_R-ELP sequence. We investigated the effects of increasing guest residue hydrophobicity and ELP length on vesicle self-assembly. The results showed that the T_t of mCherry-Z_E/Z_R-ELP protein mixtures was negatively correlated with hydrophobicity of the guest residue and ELP length. The average diameter of vesicles decreased as T_t decreased, likely due to a reduction of time spent in the transition region. Moreover, we observed formation of vesicles with properties not attainable previously by varying assembly conditions. For example, stable nanoscale protein vesicles assembled from Y$_5$-Z_R-ELP and stable microscale vesicles from Z_R-ELP$_{50}$ at physiological salt concentration. These vesicles could be used for drug delivery or artificial cell applications, respectively, in future work. This work also pointed out the importance of amphiphilic balance for stable vesicle formation. Overall, these results provide design guidance to prepare protein vesicles with desired T_t and diameter for desired applications. Such simple design rules are a unique benefit of vesicles that are not possible for traditional protein cages, which require modification of the protein–protein interfaces to alter cage size.[26,27] While protein cages have near perfect monodispersity, better than vesicles, and a wide variety of cages exist with different sizes and shapes, the ability to tune vesicle size within the same material platform lends itself to adaption for different applications. With this library of Z_R-ELP

variants, a wide variety of vesicles can now be made with globular proteins, such as enzymes or therapeutically relevant proteins fused to Z_E.[18] Additionally, vesicle size and stability can be further tuned by mixing different Z_R-ELP variants, including those with non-natural amino acids[19] or pH sensitivity,[32] or changing previous variables such as molar ratio of Z_E to Z_R,[16,18] protein concentration,[33] NaCl concentration, and warming rate.[24] This modularity and tunability will enable self-assembled protein vesicles to be applied in a range of biomedical and biotechnology applications in the future.

Experimental

Protein expression and purification

Plasmids of original Z_R-ELP, mCherry, and Z_E fragments were kind gifts from Prof. D. Tirrell at California Institute of Technology and Prof. K. Zhang at Westlake University. All plasmids of Z_R-ELP variants were purchased from Genscript. All materials and reagents were purchased from Thermo Fisher unless otherwise stated. All Z_R-ELP variants were co-expressed with His$_6$-Z_E in BL21 AF-IQ (Phe auxtroph) E. coli in 1 L of lysogeny broth containing 200 mg of ampicillin and 34 mg of chloramphenicol, induced with 1.0 mM isopropyl ß-D-1 thiogalactopyranoside (IPTG) for 6 hours at 37 °C, and harvested by centrifugation at 4000 rcf for 10 minutes. Cells were lysed using denaturing conditions in 8 M urea, 100 mM NaH$_2$PO$_4$, and 10 mM Tris·Cl at pH 8.0 and centrifuged before incubation with Ni-NTA beads (Qiagen) for at least 1 hour. Next, the samples were loaded onto a Econo-Column (BioRad) and washed with 8 M urea at pH 6.3; and Z_R-ELP variants were eluted with 6 M guanidine HCl, 100 mM NaH$_2$PO$_4$, and 10 mM Tris·Cl, as in past work.[16,18,19] Particularly, Y-Z_R-ELP variants required detergent, 5% n-octyl-ß-D-glucopyranoside, in lysis buffer. Otherwise, the cell pellet was too viscous and unable to be purified. Purified Z_R-ELPs were buffer exchanged by dialysis into Milli-Q water over 3 days by using a SpectraPor 3.5 kDa molecular weight cut-off membrane, freeze dried for long-term storage, and dissolved in water for use. As in our previous work,[16,18,19] mCherry-Z_E was expressed in BL21 AF-IQ E. coli in 1 L lysogeny broth containing 200 mg of ampicillin and 34 mg of chloramphenicol, induced with 1.0 mM IPTG then purified using Ni-NTA under native conditions. mCherry-Z_E was lysed in 10 mM imidazole, 300 mM NaCl, and 100 mM Na$_2$HPO$_4$, washed with 20 mM imidazole, and eluted with 250 mM imidazole. Lastly, mCherry-Z_E was dialyzed into phosphate buffered saline (PBS) using a SpectraPor 12–14 kDa molecular weight cut-off membrane. SDS-PAGE was used to verify the purity of all proteins. Cysteine thiols in I$_{15}$-Z_R-ELP were capped using a 10 fold molar excess of aldrithiol resuspended in methanol to ELP in water. After incubating on ice for 1 hour, modified proteins were buffer exchanged using 3 kDa centrifugal filters into cold water.

Measuring transition temperature

The turbidity, or optical density at 400 nm, of mCherry-Z_E and Z_R-ELP variant mixtures was measured every minute as temperature

6450 | J. Mater. Chem. B, 2023, **11**, 6443–6452

This journal is © The Royal Society of Chemistry 2023

increased from 5 to 40 °C using an Applied Photophysics Chirascan-plus CD UV-Vis spectrophotometer. The T_t is defined as the inflection point for a particular protein variant mixture with mCherry-Z_E and specific protein concentration, molar ratio, and salt concentration. This instrument was also used to control the heating rate during vesicle formation in specified experiments.

Characterization techniques for vesicles and other structures

Solutions were prepared on ice in 96-well plates by adding water, Z_R-ELP, mCherry-Z_E, then 10X PBS to achieve a specified salt concentration based on NaCl in 10X PBS. To induce coacervation and vesicle formation, solutions were placed at 25 °C. Turbidity was determined by measuring absorbance at 400 nm for one hour with a Biotek Instrument Synergy H4 Hybrid multimode microplate reader held at 25 °C. Size was measured using dynamic light scattering (DLS) using Malvern Instruments Zetasizer NanoZS intensity mode with a 4 mW He–Ne laser with 633 nm wavelength to detect backscattering (173°). The solvent was adjusted using the Zetasizer software to solutions containing 0.15 M, 0.30 M, 0.50 M, and 1.0 M NaCl buffered with phosphate and the material was protein. Z-average values were used to report vesicle size. Imaging of solutions was performed using an epifluorescence microscope (Zeiss Axio Observer Z1) with a 100x oil immersion lens. Transition electron microscopy (TEM) grids were prepared using 10 μL sample on copper grids and letting sample adhere for 10 minutes. Next, grids were washed with 10 μL water, negatively stained with 10 μL of 1% phosphotungstic acid, and washed again with water. Liquid was blotted from the grid using filter paper after each step then the sample was covered and dried overnight.

Author contributions

Dylan R. Dautel: conceptualization, formal analysis, investigation, writing – original draft; Yirui Li: conceptualization, formal analysis, investigation, writing – original draft; Mikaela Gray: formal analysis, investigation, writing – original draft; Michael McKenna: investigation; Julie A. Champion: conceptualization, project administration, writing – reviewing and editing.

Conflicts of interest

There are no conflicts to declare.

Acknowledgements

Notes and references

1 D. W. Urry, T. L. Trapane and K. U. Prasad, Phase-structure transitions of the elastin polypentapeptide-water system within the framework of composition-temperature studies, *Biopolymers*, 1985, **24**, 2345–2356, DOI: **10.1002/bip.360241212**.

2 A. Aghabegi Moghanjoughi, D. Khoshnevis and A. Zarrabi, A concise review on smart polymers for controlled drug release, *Drug Delivery Transl. Res.*, 2016, **6**, 333–340, DOI: **10.1007/s13346-015-0274-7**.

3 B. A. Cox, B. C. Starcher and D. W. Urry, Coacervation of Tropoelastin Results in Fiber Formation, *J. Biol. Chem.*, 1974, **249**, 997–998, DOI: **10.1016/S0021-9258(19)43030-5**.

4 D. W. Urry, Physical Chemistry of Biological Free Energy Transduction As Demonstrated by Elastic Protein-Based Polymers, *J. Phys. Chem. B*, 1997, **101**, 11007–11028, DOI: **10.1021/jp972167t**.

5 D. E. Meyer and A. Chilkoti, Quantification of the effects of chain length and concentration on the thermal behavior of elastin-like polypeptides, *Biomacromolecules*, 2004, **5**, 846–851, DOI: **10.1021/bm034215n**.

6 J. Reguera, D. W. Urry, T. M. Parker, D. T. McPherson and J. C. Rodríguez-Cabello, Effect of NaCl on the Exothermic and Endothermic Components of the Inverse Temperature Transition of a Model Elastin-like Polymer, *Biomacromolecules*, 2007, **8**, 354–358, DOI: **10.1021/bm060936l**.

7 C. H. Luan, T. M. Parker, K. U. Prasad and D. W. Urry, Differential scanning calorimetry studies of NaCl effect on the inverse temperature transition of some elastin-based polytetra-, polypenta-, and polynonapeptides, *Biopolymers*, 1991, **31**, 465–475, DOI: **10.1002/bip.360310502**.

8 D. W. Urry, *et al.*, Temperature of polypeptide inverse temperature transition depends on mean residue hydrophobicity, *J. Am. Chem. Soc.*, 1991, **113**, 4346–4348, DOI: **10.1021/ja00011a057**.

9 J. A. MacKay, D. J. Callahan, K. N. FitzGerald and A. Chilkoti, Quantitative Model of the Phase Behavior of Recombinant pH-Responsive Elastin-Like Polypeptides, *Biomacromolecules*, 2010, **11**, 2873–2879, DOI: **10.1021/bm100571j**.

10 D. W. Urry, L. C. Hayes, D. C. Gowda, C. M. Harris and R. D. Harris, Reduction-driven polypeptide folding by the $\Delta T t$ mechanism, *Biochem. Biophys. Res. Commun.*, 1992, **188**, 611–617, DOI: **10.1016/0006-291X(92)91100-5**.

11 S. A. Costa, *et al.*, Photo-Crosslinkable Unnatural Amino Acids Enable Facile Synthesis of Thermoresponsive Nano- to Microgels of Intrinsically Disordered Polypeptides, *Adv. Mater.*, 2018, **30**(5), 1704878.

12 L. Chambre, Z. Martín-Moldes, R. N. Parker and D. L. Kaplan, Bioengineered elastin- and silk-biomaterials for drug and gene delivery, *Adv. Drug Delivery Rev.*, 2020, **160**, 186–198, DOI: **10.1016/j.addr.2020.10.008**.

13 I. C. Jenkins, J. J. Milligan and A. Chilkoti, Genetically Encoded Elastin-Like Polypeptides for Drug Delivery, *Adv. Healthcare Mater.*, 2021, **10**, 2100209, DOI: **10.1002/adhm.202100209**.

14 S. R. MacEwan and A. Chilkoti, Applications of elastin-like polypeptides in drug delivery, *J. Controlled Release*, 2014, **190**, 314–330, DOI: **10.1016/j.jconrel.2014.06.028**.

This journal is © The Royal Society of Chemistry 2023

J. Mater. Chem. B, 2023, **11**, 6443–6452 | **6451**

15 A. K. Varanko, J. C. Su and A. Chilkoti, Elastin-Like Polypeptides for Biomedical Applications, *Annu. Rev. Biomed. Eng.*, 2020, **22**, 343–369, DOI: **10.1146/annurev-bioeng-092419-061127**.

16 W. M. Park and J. A. Champion, Thermally Triggered Self-Assembly of Folded Proteins into Vesicles, *J. Am. Chem. Soc.*, 2014, **136**, 17906–17909, DOI: **10.1021/ja5090157**.

17 W. M. Park and J. A. Champion, Two-Step Protein Self-Assembly in the Extracellular Matrix, *Angew. Chem., Int. Ed.*, 2013, **52**, 8098–8101, DOI: **10.1002/anie.201302331**.

18 D. R. Dautel and J. A. Champion, Protein Vesicles Self-Assembled from Functional Globular Proteins with Different Charge and Size, *Biomacromolecules*, 2021, **22**, 116–125, DOI: **10.1021/acs.biomac.0c00671**.

19 Y. Li and J. A. Champion, Photocrosslinked, Tunable Protein Vesicles for Drug Delivery Applications, *Adv. Healthcare Mater.*, 2021, **10**, 2001810, DOI: **10.1002/adhm.202001810**.

20 W. Kladwang, J. Hum and R. Das, Ultraviolet Shadowing of RNA Can Cause Significant Chemical Damage in Seconds, *Sci. Rep.*, 2012, **2**, 517, DOI: **10.1038/srep00517**.

21 D. W. Urry, *et al.*, Hydrophobicity scale for proteins based on inverse temperature transitions, *Biopolymers*, 1992, **32**, 1243–1250, DOI: **10.1002/bip.360320913**.

22 H. Arkin and M. Bilsel, How conformational transition depends on hydrophobicity of elastin-like polypeptides, *Eur. Phys. J. E: Soft Matter Biol. Phys.*, 2010, **31**, 327–332, DOI: **10.1140/epje/i2010-10573-7**.

23 J.-E. Park and J.-I. Won, Thermal behaviors of elastin-like polypeptides (ELPs) according to their physical properties and environmental conditions, *Biotechnol. Bioprocess Eng.*, 2009, **14**, 662–667, DOI: **10.1007/s12257-009-0112-1**.

24 J. N. Israelachvili, in *Intermolecular and Surface Forces*, ed. J. N. Israelachvili, Academic Press, 3rd edn, 2011, pp. 23–51.

25 D. Lombardo, M. A. Kiselev, S. Magazù and P. Calandra, Amphiphiles Self-Assembly: Basic Concepts and Future Perspectives of Supramolecular Approaches, *Adv. Condens. Matter Phys.*, 2015, 151683, DOI: **10.1155/2015/151683**.

26 J. B. Bale, *et al.*, Accurate design of megadalton-scale two-component icosahedral protein complexes, *Science*, 2016, **353**, 389–394, DOI: **10.1126/science.aaf8818**.

27 S. Tetter, *et al.*, Evolution of a virus-like architecture and packaging mechanism in a repurposed bacterial protein, *Science*, 2021, **372**, 1220–1224, DOI: **10.1126/science.abg2822**.

28 H. Nuhn and H.-A. Klok, Secondary Structure Formation and LCST Behavior of Short Elastin-Like Peptides, *Biomacromolecules*, 2008, **9**, 2755–2763, DOI: **10.1021/bm800784y**.

29 Y. Jang, *et al.*, Understanding the Coacervate-to-Vesicle Transition of Globular Fusion Proteins to Engineer Protein Vesicle Size and Membrane Heterogeneity, *Biomacromolecules*, 2019, **20**, 3494–3503, DOI: **10.1021/acs.biomac.9b00773**.

30 C. G. Claessens and J. F. Stoddart, π–π Interactions in self-assembly, *J. Phys. Org. Chem.*, 1997, **10**, 254–272, DOI: **10.1002/(SICI)1099-1395(199705)10:5 < 254::AID-POC875 > 3.0.CO;2-3**.

31 P. A. Taylor, H. Huang, K. L. Kiick and A. Jayaraman, Placement of tyrosine residues as a design element for tuning the phase transition of elastin-peptide-containing conjugates: experiments and simulations, *Mol. Syst. Des. Eng.*, 2020, **5**, 1239–1254, DOI: **10.1039/D0ME00051E**.

32 D. R. Dautel, W. T. Heller and J. A. Champion, Protein Vesicles with pH-Responsive Disassembly, *Biomacromolecules*, 2022, **23**(9), 3678–3687.

33 J. Yeongseon, *et al.*, Engineering Globular Protein Vesicles through Tunable Self-Assembly of Recombinant Fusion Proteins, *Small*, 2017, **13**, 1700399, DOI: **10.1002/smll.201700399**.

6452 | *J. Mater. Chem. B*, 2023, **11**, 6443–6452

This journal is © The Royal Society of Chemistry 2023